Nuclear Materials and Energy 39 (2024) 101630

Contents lists available at ScienceDirect

Nuclear Materials and Energy

journal homepage: www.elsevier.com/locate/nme

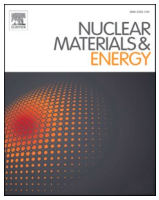

First study of the location of deuterium in displacement-damaged tungsten by nuclear reaction analysis in channeling configuration

S. Markelj [a,*], E. Punzón-Quijorna [a], M. Kelemen [a], T. Schwarz-Selinger [b], R. Heller [c], X. Jin [d], F. Djurabekova [d], E. Lu [d], J. Predrag [a]

[a] Jožef Stefan Institute (JSI), Ljubljana, Slovenia
[b] Max-Planck-Institut für Plasmaphysik (IPP), Garching, Germany
[c] Helmholtz-Zentrum Dresden-Rossendorf e.V. (HZDR), Dresden, Germany
[d] Department of Physics, University of Helsinki, Helsinki, Finland

ARTICLE INFO

Keywords:
Tungsten
Defects
Deuterium
Channeling
RBS-C
NRA-C
Displacement damage hydrogen lattice location

ABSTRACT

Nuclear reaction analysis (NRA-C) together with Rutherford backscattering spectrometry (RBS-C), both in a channeling configuration were used to study the location of deuterium (D) in irradiation-induced defects in tungsten (W) using a ^{3}He probe beam. The defects were created by W ion irradiation at two different damage doses of 0.02 and 0.2 dpa and two temperatures of 290 K and 800 K. Angular scans over the ⟨1 0 0⟩ axial channel showed that for both 800 K irradiated samples the NRA yield peaks in the centre of the channel, where the RBS is at its minimum. For the room-temperature-irradiated samples this is only true for the low dose. For the high dose sample hardly any peak is observed. 2D channeling maps were recorded for the samples damaged to 0.02 dpa at 290 K and 0.2 dpa at 800 K. They show in addition to the maximum D signal in the ⟨1 0 0⟩ axial channel increased intensity in a (1 1 0) planar channel where the RBS intensities are low. The software algorithm RBSADEC was used to investigate the location of the D in the lattice. A first comparison of simulation and experiment suggests that D is located close to tetrahedral sites.

Introduction

Understanding the interaction of hydrogen with the host lattice of both plasma-facing (PF) and structural materials is crucial for fusion research, since low hydrogen isotope (HI) retention is a stringent requirement for a fusion reactor. Existing experiments and state-of-the-art theory and modelling cannot satisfactorily describe the interaction of hydrogen with large structural defects that will be created by 14 MeV neutron irradiation, nor can they yet account for the possible synergistic effects of the presence of HIs on defect evolution. In future fusion reactors, one of the main material candidates for the plasma-facing surface is tungsten (W), because of its favourable properties such as high melting temperature, high thermal conductivity and low intrinsic retention of HIs. However, in a future fusion environment, the 14 MeV neutrons from the D-T fusion reaction will create defects in the crystal lattice, degrading, e.g., thermal conductivity and increasing fuel retention.

In this work, we show first results of the development of an advanced characterisation technique. By combining different ion beam techniques in the channeling configuration, the influence of structural defects on HI retention and vice versa is studied. To characterize the generated defects in the tungsten sample, we use Rutherford backscattering spectrometry in the channeling configuration (RBS-C). It is a well-established method to study the crystal structure of materials, in particular the lattice disorder and defect evolution induced by ion irradiation. To quantify the disorder, the change in the ion yield of the backscattered ions along a specific crystallographic direction is measured [1,2]. To detect light elements in the matrix, nuclear reaction analysis is often used. Here, we combine NRA in the channeling configuration (NRA-C) in conjunction with RBS-C to provide information on the location of light elements in the host material [1]. In our case, we use the ^{3}He nuclear reaction with deuterium to study the location of deuterium in the tungsten lattice. Pioneering studies on the location of deuterium in several single crystals (W, Cr, Fe, Ni and W) were carried out in the 1980 s by Picraux and Myers at Sandia National Laboratories (SNL) using a combination of NRA-C and RBS-C [3,4,5]. As recently shown [6] by re-evaluation of their measurements [4], the location of deuterium in tungsten in this early work was influenced by the creation of defects with the 30 keV D ion implantation and by the presence of the analysing helium in the

* Corresponding author.
E-mail address: sabina.markelj@ijs.si (S. Markelj).

https://doi.org/10.1016/j.nme.2024.101630
Received 10 November 2023; Received in revised form 8 February 2024; Accepted 29 February 2024
Available online 1 March 2024

lattice. In this work, we apply also NRA-C and RBS-C but with a different experimental approach: First, we do not apply it to pristine tungsten crystals but to displacement-damaged tungsten. Second, the ambiguities of the original works are avoided by using low energy D to decorate the displacement damage. In addition, the simulation of C-RBS and C-NRA spectra with the state-of-the-art code RBSADEC [7] and comparison with the measured spectra will allow to investigate the influence of different structural defects on deuterium location and retention. The present manuscript reports on the experimental strategy and first experimental results about the location of D in displacement-damaged tungsten to reflect the status as presented at the 21st International Conference on Fusion Reactor Materials (ICFRM-21). At present, a combined C-RBS and C-NRA experiment is being set up at Jožef Stefan Institute (JSI), Ljubljana, Slovenia in a refined fashion and the application of the presented methodology on displacement-damaged tungsten is the focus of our future work.

Experiment

Sample preparation

All preparation steps such as sample polishing, annealing, W irradiation and D loading were performed at the Max-Planck-Institut für Plasmaphysik (IPP), Garching, Germany. Tungsten (W) single crystal (SC) samples with surface orientation (1 0 0) and dimensions of 1x10x10 mm^3 from MaTecK were used. The crystals had a purity of 99.999 % and a surface normal orientation with an accuracy of $< 0.1^\circ$. The top surface was polished to an average roughness Ra $<$ 10 nm. Initial scanning electron microscopy (SEM) characterisation of the as-received samples revealed surface distortions, such as surface scratches and grooves, resulting from mechanical polishing. Therefore, an additional chemo-mechanical vibration-polishing process was applied. The quality of the final samples was assessed by characterization of the surface by classical SEM and in addition by SEM-based electron channeling contrast imaging (ECCI), which produces a Kikuchi-like pattern that is strongly dependent on the crystal structure of the single crystal sample. While the samples did not show any pattern in their as-delivered state, after vibration-polishing, clear channeling patterns demonstrated that the surface had been properly prepared. After the polishing, the samples were high-temperature annealed by electron beam heating for 5 min at 2350 K with a slow cooling ramp at a pressure $< 5{\cdot}10^{-8}$ mbar.

In order to study the defects and trapping of deuterium by RBS-C and NRA-C, four tungsten (1 0 0) single crystals were irradiated with 10.8 MeV W^{3+} ions at two different W fluences of 5.8×10^{16} m^{-2} and 5.8×10^{17} m^{-2}, respectively, and at two different temperatures of 290 K and 800 K. The W beam was scanned vertically and horizontally with about 1 kHz (beam dimensions of 2.5 mm, full width at half maximum). The average damage rate was 2×10^{-4} dpa/sec. Peak damage rate was 100 times larger. The "Ion Distribution and Quick Calculation of Damage" calculation option of the SRIM 2008.04 code [8] was used to calculate the depth profile of the primary damage. A displacement energy of 90 eV [9] was used and the "vacancy.txt" output was evaluated. The damaged zone extends down to 1.3 μm, with a peak damage of 0.02 or 0.2 dpa at 0.6 μm for the W fluences stated above. W ion irradiation was performed with a 7° tilt and 6° rotation to minimize unwanted ion channelling during irradiation. The aim was to create specific microstructural defects in the tungsten SC, with either single vacancies or small or large vacancy clusters dominating the material [10]. Such open volume defects are known to act as trapping sites with high de-trapping energy for hydrogen isotopes [3]. In [10] they mainly focused on the characterization of vacancy-type defects; however, as shown in [11,12], self-interstitial-type defects such as dislocation loops and lines are also present in the samples after W irradiation. At low dpa irradiation conditions, dislocation loops are expected to be dominant in the material [11,12], whereas at high dpa it has been shown in [9] that numerous dislocation lines are formed, replacing dislocation loops as the dominant visible defect. This was confirmed in our recent study on W (1 1 1) SC samples prepared in the same way as described above [13]. One sample was left unirradiated to have a pristine reference.

The W ion irradiated tungsten SC samples were additionally exposed to a plasma at 370 K with a D ion energy of 5 eV/D and a D ion flux of 6×10^{19} D/m^2s for 48 h, resulting in a D ion fluence of 1×10^{25} D/m^2. From previous experience, this fluence was sufficient to populate the defects with deuterium throughout the whole damage depth [14].

Calculations show that for the W (1 0 0) SC a clear difference in the NRA-C signal is expected when deuterium is close to the octahedral interstitial sites (OIS) or tetrahedral interstitial sites (TIS) [15]. It is important to note, there is hardly any difference visible in the NRA-C yield for W (1 1 1) SC [1,15] used in our previous study [13] and for this reason we changed for this study to the W (1 0 0). However, the created defects in the samples are the same, no matter the surface orientation.

Positron annihilation lifetime spectroscopy (PALS) was performed at University of Helsinki, Finland on W SC samples with surface orientation (1 1 1), prepared in the same way [13] than the above described W (1 0 0) SC samples but without decorating them with D. For this purpose, a digital coincidence lifetime spectrometer, which has a time resolution of 220 ps (FWHM), was used. A positron source (^{22}Na wrapped in 1.5 μm thick Al foil) was sandwiched between a pristine (2325 K annealed) and W-irradiated tungsten single crystal samples. The results can be used here to characterize the open volume defects created by the W irradiation.

Experimental set-up

Tungsten SC samples decorated with D plasma were analysed with RBS-C and NRA-C at the multi-detector RBS system at Helmholtz-Zentrum Dresden-Rossendorf (HZDR), Rossendorf, Germany, the so-called Hedgehog system. This set-up is attached to the ion beam center's 3 MV tandetron accelerator. It basically consists of 76 individual Si detectors arranged in 5 concentric rings around the sample. These 5 rings contain 6, 12, 16, 20 and 22 detectors, respectively. All detectors within a ring have the same scattering angle of 165°, 150°, 135°, 120° and 105°, respectively. Each detector has a solid angle of 8.9 msr so that in total a solid angle of 676 msr is covered. Fig. 1 shows a schematic sketch and a photo of the set-up.

As each detector is connected to its own spectroscopic electronics (pre-amplifier, spectroscopic amplifier, analogue-to-digital converter (ADC) and multi-channel analyser (MCA)), the entire system can operate at a count rate of up to 8 mega counts per second without significant pile-up effects. For channelling experiments, the target chamber of the setup is equipped with a high-precision 5-axis goniometer. It allows the sample to be tilted in the horizontal (angle tilt) and vertical (angle theta) direction by +/-8° with an accuracy of 0.01°. The large solid angle allows the acquisition of 2D channeling maps on a time scale of minutes, even at low ion beam intensities below 1 nA.

The first set of measurements was performed with a 2.5 MeV ^{4}He beam to find the ⟨1 0 0⟩ axial channel and other planar channels by RBS-C. Later, to make NRA-C, we switched to a ^{3}He beam to employ the D(^{3}He,p)^{4}He nuclear reaction. Using a 800 keV ^{3}He beam, we were able to resolve the signal from the backscattered ^{3}He on tungsten and the proton and alpha signal from the nuclear reaction with the same detectors previously used for RBS. According to SRIM, the maximum range of the 800 keV ^{3}He ions in an amorphous W target is 1.06 μm. For this primary ^{3}He energy the maximum in the D(^{3}He,p)^{4}He cross section is reached at a depth of 270 nm (600 keV energy) [16]. In this respect one needs to be aware that the ions are in a channeling configuration meaning that the actual ion range is larger [17] than the SRIM calculation. As the damage depth of the 10.8 Me W ions is much larger than this depth (1.3 μm compared to 270 nm) NRA can be applied but quantification of the depth scale will be affected by channeling. Fig. 2 shows the ion yield collected with the detectors at 165 and 135°, obtained with a 800 keV

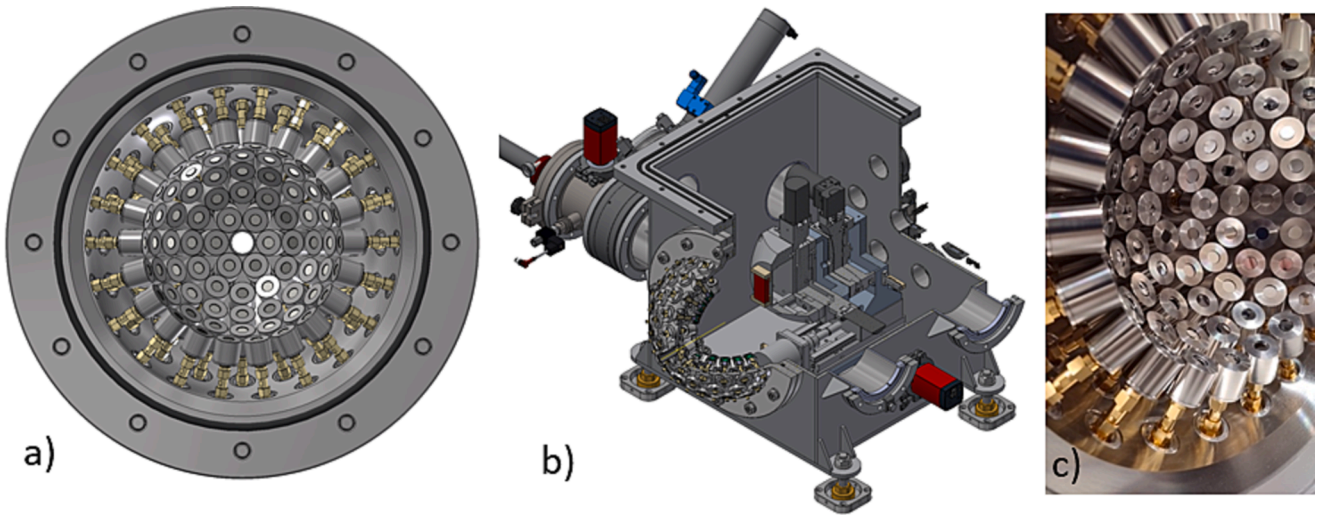

Fig. 1. A) schematic sketch of the detector set-up and b) the detector set-up mounted on the experimental chamber. c) photograph of the detector set-up.

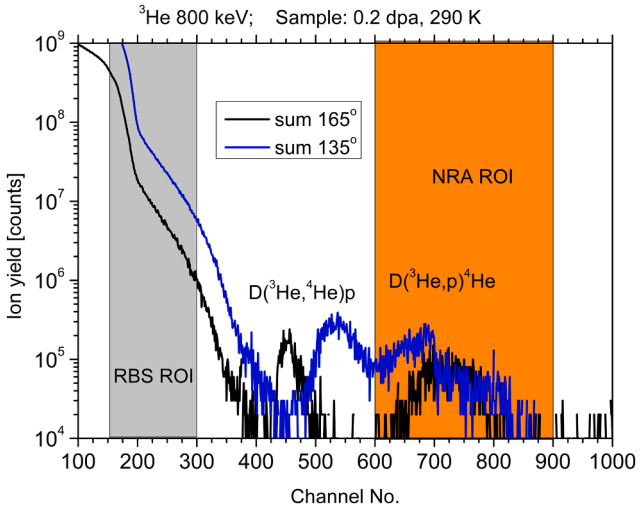

Fig. 2. Spectra measured with a 800 keV ^{3}He beam on the 0.2 dpa / 290 K sample for two different scattering angles of 165° and 135°. The ROIs for RBS and NRA are marked. The left shoulder is due to backscattered ^{3}He ions, the signals to the right stem from the alphas and the protons from the nuclear reaction.

^{3}He beam on the 0.2 dpa / 290 K sample. One can observe a shoulder on the left side which is due to backscattered ^{3}He ions (RBS signal). The peaks on the right are due to protons and alphas from the nuclear reaction (NRA). The RBS signal is orders of magnitude larger than the NRA but they are well separated for this ^{3}He energy. It is important to note that the high-energy protons (12–13 MeV) from the nuclear reaction deposit only a part of their energy in the about 350 μm thick silicon detectors. Therefore, the primary He energy has to be chosen carefully to be able to separate the NRA signal from the RBS signal in the same detector. For instance, at 1.2 MeV ^{3}He energy the RBS pile-up signal was already interfering with the NRA signal and the two signals could not be resolved. Identification of the peaks was done by the help of spectra simulation by the SIMNRA program [18] introducing the proper detector thickness and scattering data. When plotting intensity maps for RBS-C and NRA-C, for instance angular scans or 2D channeling maps, we plot the integrated signal from a certain region of interest (ROI). For RBS-C and NRA-C we chose different ROI. The region of interest for NRA was chosen based on a measurement of a deuterium standard which was in our case a thin amorphous deuterated carbon (a-C:D) layer deposited on a silicon wafer [19] and rechecked on the 0.2 dpa / 290 K sample. In Fig. 2 the respective ROIs are shown. The signal from the alpha particles is shifting depending on the angle and gets close to the RBS signal. For this reason, the NRA ROI was selected to be in the energy region where mainly protons from the nuclear reaction were detected. For RBS, we integrated over 150 energy channels, between energy channel 150 and 300. For each measurement where a 2D map was performed, the sample was moved varying theta and tilt angles. At each theta and tilt, the spectra were collected and the integral under the selected ROI, for each spectrum, was added, normalized to the current and plotted as an intensity in the 2D plot. After each measurement set the sample was moved to a different lateral position. The measurement of the signal was made such that for each point the time the goniometer spent in an individual angle step was constant. The signal obtained in that time was then normalized to the average beam current. It is important to note that with this set-up it is not possible to determine the absolute D concentration and the D depth profiles since the protons from the nuclear reaction deposit only part of their energy in the detector. In order to derive absolute quantities and D depth profiles one needs to stop the protons completely and the energy distribution of the proton spectra is analysed [20]. In addition, spectra with different ^{3}He energies need to be collected as demonstrated in [20] which could not be performed at HZDR. For this reason, for a standard D depth profile measurement, samples were additionally analysed at IPP, Garching using nine ^{3}He energies [14]. Samples were rotated by 14° in theta and 15° in phi for this measurement to minimize axial and planar channeling.

Simulation

To gain insight into the location of deuterium within the lattice of the irradiated W samples, the RBS-C and NRA-C experiments were simulated using the RBSADEC (RBS from Arbitrary DEfected Crystals) code [7,21]. This code allows the generation of RBS-C spectra from targets containing arbitrary atomic structures, generated from molecular dynamics simulations [13].

Recently, the RBSADEC code has been upgraded to simulate not only RBS-C but also NRA-C spectra [6]. For the NRA-C simulations presented here, ^{3}He ions were used to probe the tungsten target along the ⟨001⟩ direction. In all the simulations, the detector was located at 135 degrees to detect the emitted protons from the nuclear reaction D(^{3}He,p)^{4}He. The differential cross section from [16] was used. For incident beam divergence, the angular distribution of incoming ions was set to follow a Gaussian distribution with a standard deviation of 0.06 degree.

Results and discussion

We performed 2D channeling maps on a pristine W (1 0 0) SC sample and on the W (1 0 0) SC samples irradiated under different conditions, by changing theta and tilt angles. Fig. 3a shows the 2D RBS-C channeling map obtained on a pristine W SC sample with a 2.5 MeV ^{4}He ion beam while varying the theta and tilt angle by ± 2°. The signal of all detectors was summed in this and in all other cases later. A broad circular minimum RBS signal at theta = 0.8° and tilt = 1° is visible and saddles going radially outward from the deep valley. The shift in the theta and tilt from 0° gives the sample surface misalignment w.r.t. the (1 0 0) plane. Fig. 3b shows RBSADEC simulations of the RBS-C yield obtained with 2.5 MeV ^{4}He ions to probe the tungsten target along the ⟨0 0 1⟩ direction. The detector resolution for the RBS-C simulations is 15 keV. Comparing the RBS intensities, we were able to determine that the deep valley is the axial channel in the ⟨1 0 0⟩ direction and the observed saddles are the (1 1 0) and (1 0 0) planar channels, as marked in Fig. 3. The agreement between the experiment and the simulation is excellent. The RBS yield minima and saddles are well reproduced.

Fig. 4 shows two 2D RBS channeling maps with a 2.5 Me ^{4}He beam obtained on W-irradiated W (1 0 0) SC samples. The map for the 0.2 dpa / 290 K sample is shown in Fig. 4a. The map for the 0.2 dpa / 800 K sample is shown in Fig. 4b. In the case of W-irradiated samples, we have varied the theta and tilt by ± 2.5°. For the 0.2 dpa / 290 K sample the axial channel and the planar channels are not as deep and wide as compared with the pristine W SC (Fig. 3). This is in line with the larger damage created in the sample that leads to dechanneling. The 0.2 dpa / 800 K sample showed clearer and wider channels in the RBS yield compared with the 0.2 dpa / 290 K sample, even though the damage dose is the same. This suggests that fewer defects are created in the 0.2 dpa / 800 K sample due to the higher irradiation temperature. This is in line with deuterium retention results for similar damaging conditions [22,23] and to the retention measurements shown later and can be explained by the fact that vacancies can move and annihilate with other defects at 800 K [24]. A more detailed analysis of the RBS-C measured spectra together with simulations using the RBSADEC code was performed on W (1 1 1) SC samples irradiated at 290 K to 0.02 dpa and 0.2 dpa in [13]. There molecular dynamics (MD) simulations of

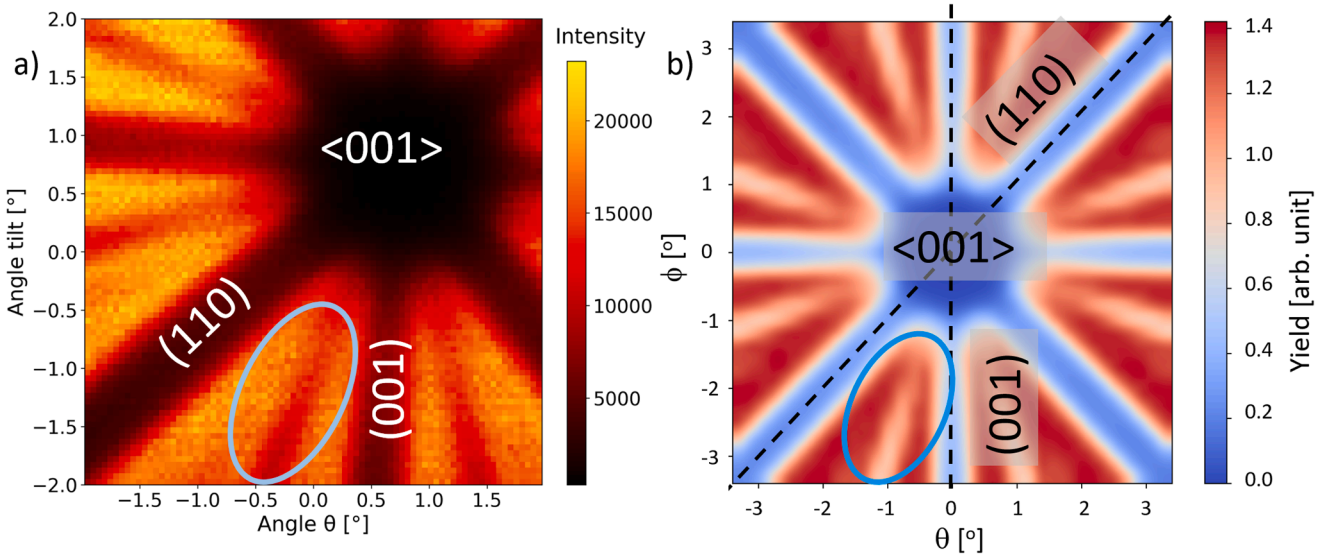

Fig. 3. Measured (a) and simulated (b) RBS-C 2D maps of the RBS yield as a function of theta and tilt angle on a pristine, non-damaged (1 0 0) W single crystal. The spectra were obtained with a 2.5 MeV ^{4}He beam.

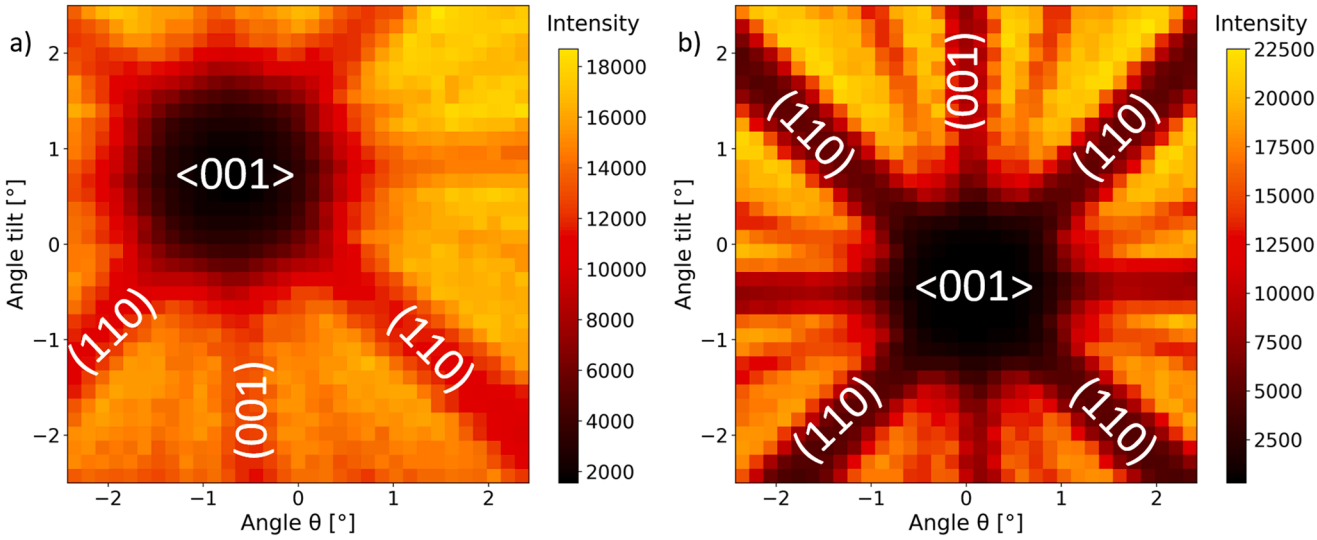

Fig. 4. C-RBS 2D maps measured with a 2.5 MeV ^{4}He beam of the 0.2 dpa irradiated W (1 0 0) SC samples W-irradiated at 290 K a) and at 800 K b).

overlapping cascades were used as input.

As mentioned before, in order to study the location of deuterium in W-irradiated samples, we performed NRA-C measurements with a ^{3}He beam at 800 keV energy. The NRA-C spectra were measured simultaneously with the RBS-C yield. The scanning area was shifted so that the ⟨1 0 0⟩ axial channel was in the centre. The shift angle for tilt and theta were obtained from the 2D scans using the 2.5 MeV ^{4}He beam. The signal of all detectors was summed for the 2D maps and angular scans. Figs. 5 and 6 show 2D RBS-C and NRA-C maps measured on the 0.2 dpa / 800 K and 0.02 dpa / 290 K samples, respectively. In the case of RBS-C, the 2D channelings maps are very similar to that obtained with the 2.5 MeV ^{4}He beam shown in Fig. 4. In contrast to the RBS-C spectra, where we got a decrease of the RBS signal in the axial and planar directions, we obtained an increased NRA signal in the ⟨1 0 0⟩ axial channel and along the (1 1 0) planar channels for both samples studied. Due to the limited beam time, 2D maps for the other two samples (0.2 dpa / 290 K and 0.02 dpa / 800 K) could not be measured.

In Fig. 7, angular scans across the ⟨1 0 0⟩ axial channel and along the (1 0 0) planar channel are shown for all four W-irradiated samples. According to [10] the 0.02 dpa / 800 K sample contains mainly small vacancy clusters and the 0.2 dpa / 800 K sample mainly large vacancy clusters. On the other hand, the 0.02 dpa / 290 K sample should contain mainly single vacancies [10]. The 0.2 dpa / 290 K is expected to contain both single vacancies and large vacancy clusters according to deuterium retention analysis [23]. This was confirmed also with positron annihilation spectroscopy performed on W (1 1 1) SC samples prepared in identical fashion. It is important to note that a single vacancy can at room temperature store up to 6 hydrogen atoms [25,26,27], while different sizes of vacancy clusters can store even more hydrogen atoms [27]. It was recently shown [6] that for a single hydrogen atom in a vacancy, it would appear in NRA-C as if the hydrogen would be sitting close to the OIS. As the hydrogen fill level is increased, the hydrogen location moves towards the direction of the TIS. For a fill level of 6, the NRA yield looks like hydrogen atoms are distributed around the midpoint of the OIS and TIS. To the authors's knowledge, there was no such detailed study yet carried out for vacancy clusters. For our exposure conditions (at 370 K) vacancies should be filled with up to 5 atoms [28].

Fig. 7 shows two data sets for the 0.2 dpa / 800 K sample and for the 0.02 dpa / 290 K sample. The first one is obtained from a single angular scan over the theta angle, while the second one is extracted from the 2D maps shown in Figs. 5 and 6. The main difference in the angular scans between the samples is that the peak for the samples irradiated at 800 K has a wider and higher NRA signal compared with the 0.02 dpa / 290 K sample. This could be due to the fact that the vacancy clusters are larger in size and the deuterium location in these clusters has a broader distribution, further away from the centre of the cluster. The difference in the NRA-C yields is probabaly not due to the fill level of D atoms in a mono-vacancy or in vacancy clusters. Fig. 7 also shows the angular scan for the 0.2 dpa / 290 K sample, which shows only small peak in the NRA signal. This can be interpreted as the deuterium being trapped in various

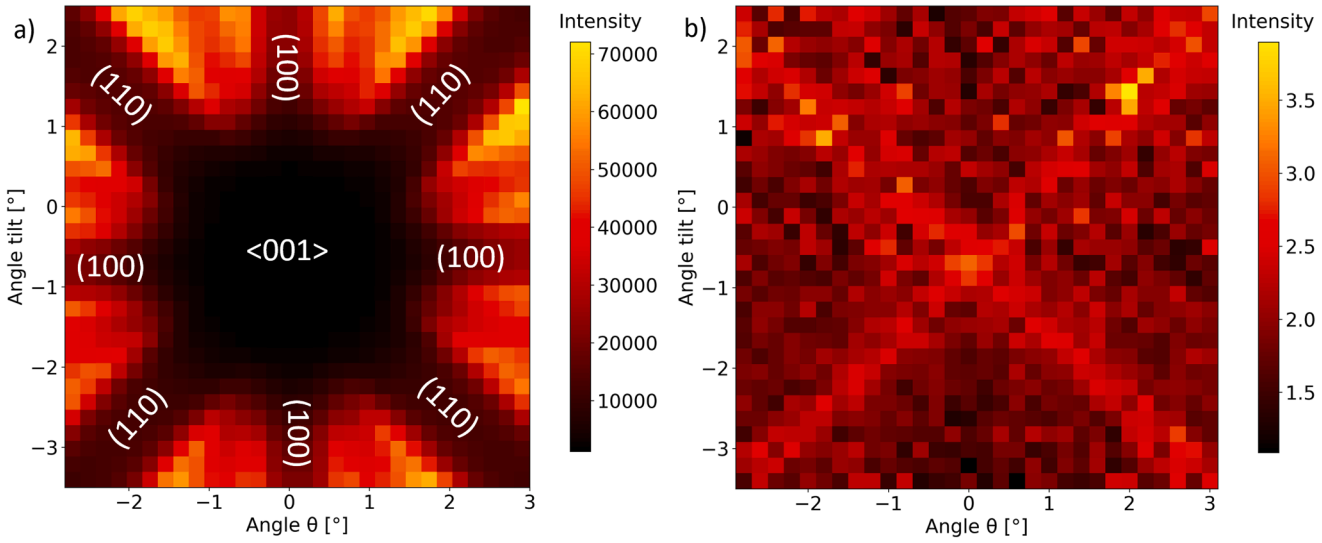

Fig. 5. 2D maps of the 0.2 dpa / 800 K sample measured with a 0.8 MeV ^{3}He beam as a function of theta and tilt angle: a) RBS yield. b) NRA yield. The ⟨1 0 0⟩ axial channel and the (1 0 0) and (1 1 0) planar channels are marked in the left figure.

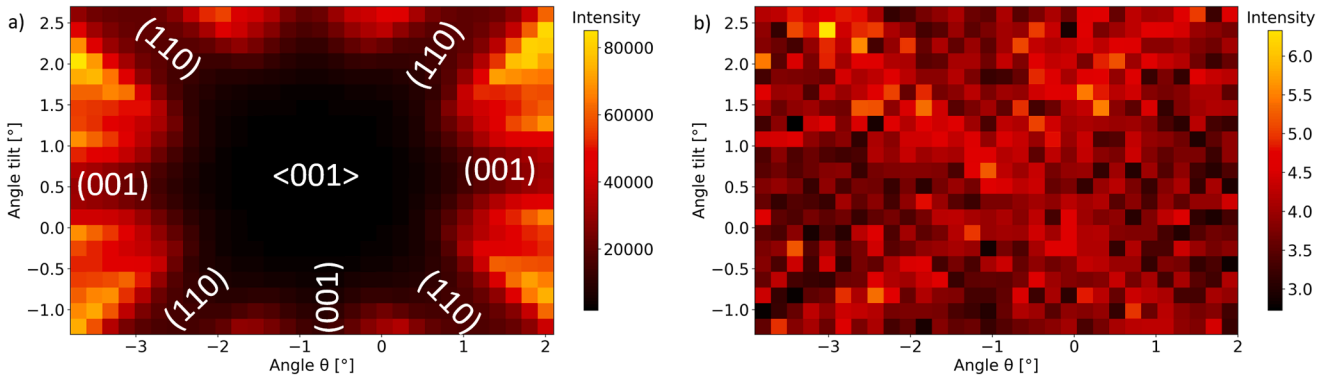

Fig. 6. 2D maps of the 0.02 dpa / 290 K sample measured with a 0.8 MeV ^{3}He beam as a function of theta and tilt angle: a) RBS yield. b) NRA yield. The ⟨1 0 0⟩ axial channel and the (1 0 0) and (1 1 0) planar channels are marked in the left figure.

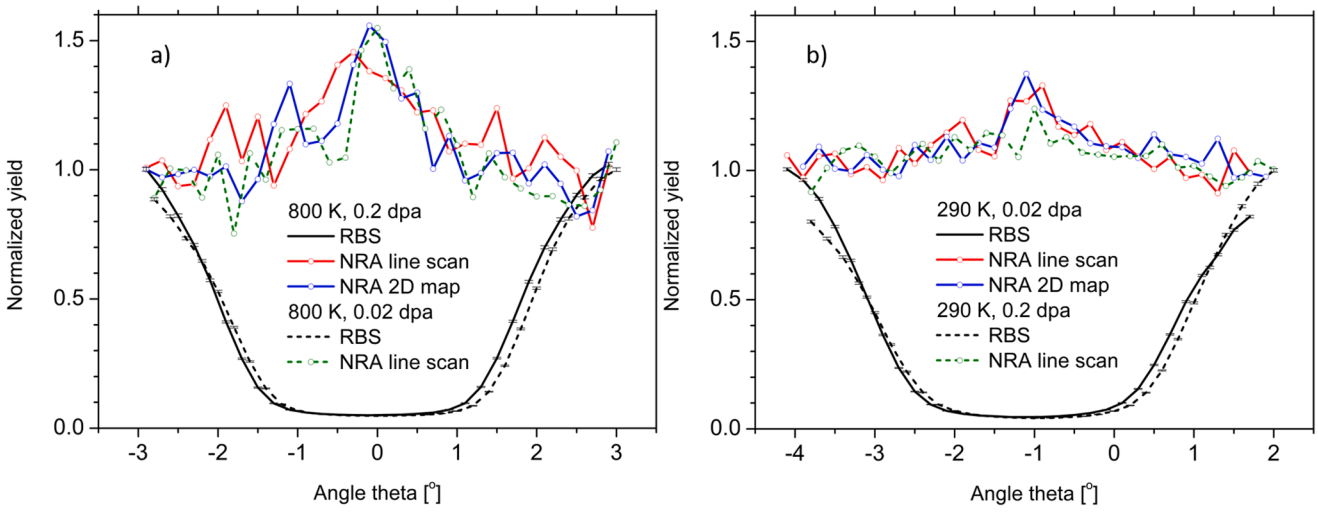

Fig. 7. Normalised RBS (black line) and NRA (red, blue and olive lines with dots) yields as a function of theta angle are shown for W (1 0 0) SC samples irradiated at 0.2 dpa and 0.02 dpa at 800 K a) and at 290 K b).

defects such as vacancies and vacancy clusters which could smear the NRA signal. Smearing out of the deuterium signal at large damage doses was already shown and discussed in the old measurements in the 1980's [3].

The data shown in Fig. 7 were normalized and the normalization values reflect the general D retention in these samples. Namely, the normalization constants for NRA were 19.5 and 10.5 for samples with 0.2 dpa and 0.02 dpa damaged at 290 K and 4.7 and 3 for samples with 0.2 and 0.02 dpa damaged at 800 K, respectively. Due to the very low signal for NRA, the statistical error bars are of the order of 50–80 %. For clarity of the image they are not shown. The quantitative D depth profiles obtained from these samples at IPP, Garching are shown in Fig. 8. The D concentration is the highest for the 0.2 dpa / 290 K sample with 1.55 ± 0.03 at. % at the maximum. The sample damaged to 0.02 dpa at 290 K shows a lower D concentration of 0.62 ± 0.02 at. %. The D concentrations for the samples damaged at 800 K are even lower with 0.36 ± 0.02 at. % and 0.18 ± 0.02 at. % for damage doses of 0.2 and 0.02 dpa, respectively. The increased D concentration is observed down to about 1.5 μm which is in good agreement with the SRIM-calculated damage depth. Beyond this depth the D concentration steadily decreases below 10^{-3} at. % which is a typical level for unirradiated W [14]. The concentrations agree very well with similar irradiations of recrystallized polycrystalline tungsten samples performed at identical temperatures and dose [22,14]. The trend of the maximum D concentrations from these depth profiles agrees with the normalization constants obtained for the C-NRA linear scans. We can conclude that higher irradiation temperature and lower damage dose results in smaller D concentration meaning also less defects. It is important to note that the height of the central peaks in the linear scans of the NRA-C yield do neither reflect the expected trend of the damage dose nor the one for the irradiation temperature. For this reason, we believe, that these peaks reflect the local distribution of D around the open volume defect. In the case of a single vacancy, the energetically most favorable positions D atoms were found to be at octahedral sites, on faces of the primary cell [25,6]. This means they are not dominantly in the channel where the probability for the nuclear reaction is high. On the other hand, in the case of vacancy clusters the objects are bigger and according to [27] D atoms are adsorbed on the surfaces of vacancy clusters or nanovoids. For this reason, the chance that the D atoms are localized in the channel is larger and for this reason also higher peaks are visible.

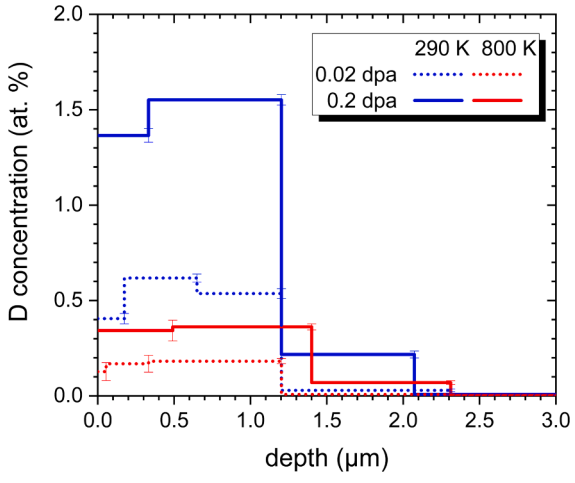

Fig. 8. D concentration depth profiles as obtained on the different W-irradiated W (1 0 0) SC samples.

In order to characterize the open volume defects in our samples, we performed PALS on W (1 1 1) SC samples prepared the same way as samples the W (1 0 0) SC samples for the NRA-C study (except for the final D decoration of defects with D). Compared with the reference pristine sample, all spectra obtained on these W-irradiated samples showed clearly longer lifetime components, which are attributed to the production of irradiation-induced open-volume defects. The exponential decay analysis was performed on all positron lifetime spectra in order to quantify the positron annihilation lifetime parameters. The lifetime spectrum for the pristine single crystal sample could be described with only one single lifetime component with a bulk value $\tau_B = 108.4$ ps. This value is consistent with the values of positron annihilation lifetime in defect-free tungsten (100 – 110 ps) reported in the past [29,24]. Two-component analysis was performed on positron lifetime spectra measured on W-irradiated samples. The analysed values of the longer lifetime component (τ_2) unveil the size information of defects in different samples. In previous publications, the positron annihilation lifetime value for a mono-vacancy in tungsten was determined to be in the range 160 – 200 ps [24,29]. For the 0.02 dpa / 290 K irradiated sample, the lifetime τ_2 of 224 ± 30 ps suggests vacancy defects larger than a mono-vacancy (V) being dominantly produced. From the results observed for the 0.2 dpa / 290 K sample, the value of τ_2 of 265 ± 8 ps suggests even larger increase of the vacancy size. We speculate that small vacancy clusters were formed with the size V2 - V4 based on the theoretical data [29]. For the high temperature (800 K) irradiated

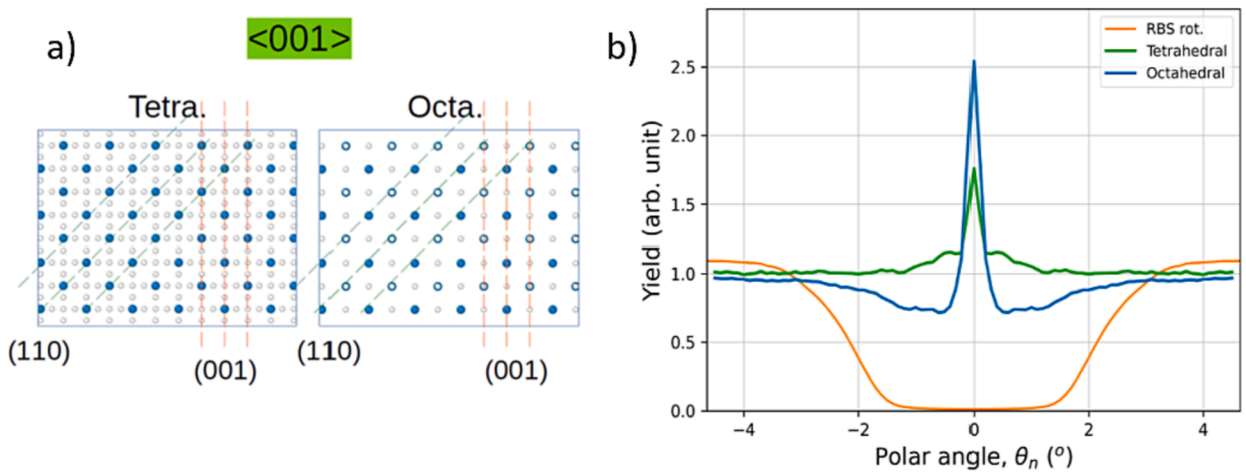

Fig. 9. a) the crystal structure of W SC for the ⟨001⟩ axial orientation. Blue dots are W atoms and white dots are deuterium atoms. b) RBS-C and NRA-C yield as a function of angle theta, NRA-C scans are calculated for deuterium located at TIS or the OIS location.

samples, the values of τ_2 were higher than 400 ps regardless of the irradiation dose, 429 ± 8 ps and 453 ± 3 ps for damage dose of 0.02 and 0.2 dpa respectively, indicating large vacancy clusters with an estimated size of more than 25 vacancies. This confirms our initial expectations of producing different microstructures by increasing the irradiation temperature from room temperature to 800 K. The PALS results also confirm our speculation regarding the possible difference of the D location in the different samples.

In order to additionally understand the measured 2D NRA-C yield and angular scans, initial simulations were performed using the RBSA-DEC code [7,6]. As a first assumption for the simulation of the NRA-C maps and angular scans, for comparison with the experiment, we considered two extreme cases: deuterium located at TIS and OIS. At this stage no defects were added in the simulations. Deuterium was placed only at specific locations. Fig. 9a shows the crystal structure with W atoms and D atoms at TIS or OIS in the direction of the ⟨001⟩ axial channel. The (110) and (001) planar channels are also marked. Fig. 9b shows the simulated RBS and NRA yields as a function of the theta angle. The ^{3}He energy in Fig. 9b was 750 keV and the detector resolution was set to 16.5 keV. The NRA-C and RBS-C simulations are used to show the difference of TIS and OIS. The simulation temperature and the Debye temperature of the tungsten targets were 290 K and 377 K, respectively [30], which gives a 1D thermal vibration magnitude of tungsten atoms equal to 4 pm. The 1D thermal vibration magnitude of D atoms was set to 14 pm [1]. The NRA-C simulations in Fig. 10a and 10b are used to compare with the experimental 2D scans, in which the energy of ^{3}He ions is 800 keV. In the first case D was placed at TIS (Fig. 10a) and in the second case the lattice location of D atoms is determined according to the position of one D atom in one mono-vacancy, which is close to OIS, but not exactly at OIS (Fig. 10b). It is displaced by 0.10 Å from the OIS towards the TIS, and has a distance of 0.32 Å with the closest vacancy surface, where the vacancy surfaces here refer to the 6 faces of the unit cell. One can clearly observe a difference between the NRA yields in the 2D maps for the two cases. A quantitative comparison with the experimental data shown in Fig. 7 is at this stage not yet possible because at this stage no large defects were added in the simulations. However, it looks like that the angular scans and 2D maps are more similar to spectra where the D is located close to TIS.

Conclusion

Four W (100) SC samples were irradiated with 10.8 MeV W ions at two different damage doses (0.02 dpa and 0.2 dpa) and two temperatures (290 K and 800 K) to create different empty-volume type defects in the material and to study the trapping of deuterium at such defects. For this purpose, we have for the first time used NRA-C simultaneously with RBS-C using a ^{3}He probe beam to study the location of deuterium in displacement-damaged W. Maximum signal was obtained in the ⟨100⟩ axial channel and in the (110) planar channel for the samples irradiated at 0.2 dpa at 800 K and at 0.02 dpa at 290 K. Angular scans over the ⟨100⟩ axial channel showed that, for both samples irradiated at 800 K, the NRA yield peaks in the centre of the channel, where the RBS is at its minimum. For the samples irradiated at 290 K this is only true for the low dose, while for the high dose sample hardly any peak was observed.

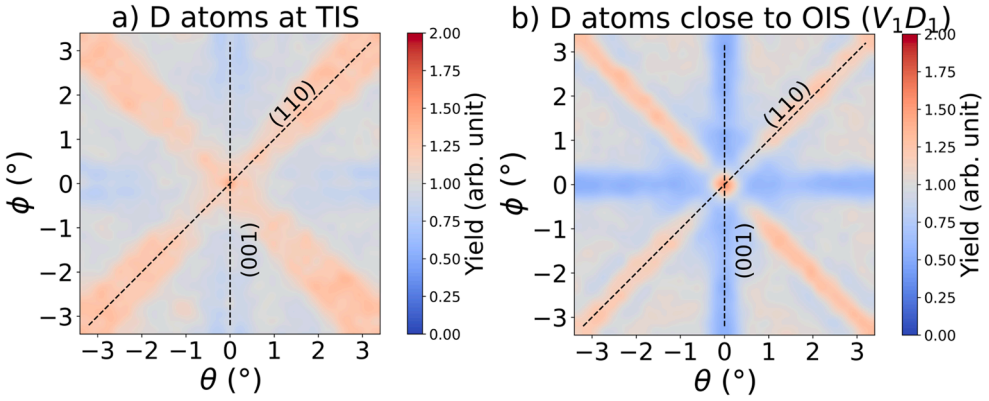

Fig. 10. 2D NRA maps as a function of theta and tilt for deuterium located at a) TIS and b) at the position as if one D atom would be in one mono-vacancy, which is close to OIS.

The integrated NRA signal is reflecting the D concentration in the damaged region whereas the intensity distribution of the NRA-C yield of the angular scan gives information about the D location in the lattice around different defects. Separate additional non-channeling D retention measurement showed that the highest D concentration was obtained for the sample damaged at 290 K to a damage dose of 0.2 dpa. The D concentration decreases for lower damage dose and also for higher irradiation temperature of 800 K, meaning that less defects are created at lower dose and at higher temperatures. The nature of the defects was analyzed by PALS showing that for samples irradiated at 290 K mainly single vacancies and small vacancy clusters up to V4 are present, whereas for samples irradiated at 800 K large vacancy clusters are present with more than 25 vacancies. It was also observed that the peak in the NRA-C yield of the angular scan measurement is broader for samples irradiated at 800 K, which we suspect is due to the presence of vacancy clusters. The NRA peak is smaller and narrower for samples irradiated at 290 K. A first qualitiative comparison was performed with simulations using the RBSADEC code. At the present stage we cannot yet simulate the defects populated by D in the lattice but we simply placed D at certain interstitial positions. Still the first comparison indicates that NRA yields for the angular scans are similar to the measured ones when D is positioned at the TIS. For a more detailed comparison, RBSADEC simulations in combination with density functional theory to study the location of hydrogen in vacancies and vacancy clusters need to be performed and are planned for the future. We have shown in this paper the first scoping study whether NRA-C can be applied to study the deuterium location in materials containing structural defects. Compared to neutron diffraction (ND), which is an established technique to determine the location of hydrogen in compounds, e.g. in hydrogen-energy materials [31], much smaller amounts of hydrogen are needed in the structure (here from 0.5 to 1.8 at. % within only 1 micrometer compared to about 30 at. % in milimeter size samples for ND). However further studies are needed to probe NRA-C sensitivity and limitations.

CRediT authorship contribution statement

S. Markelj: Conceptualization, Formal analysis, Investigation, Resources, Visualization, Writing – original draft, Writing – review & editing. **E. Punzón-Quijorna:** Investigation, Writing – review & editing. **M. Kelemen:** Investigation. **T. Schwarz-Selinger:** Investigation, Resources, Writing – review & editing. **R. Heller:** Investigation, Resources, Writing – review & editing. **X. Jin:** Investigation, Software, Visualization, Writing – review & editing. **F. Djurabekova:** Resources, Software. **E. Lu:** Formal analysis, Investigation. **J. Predrag:** Visualization.

Declaration of competing interest

The authors declare that they have no known competing financial interests or personal relationships that could have appeared to influence the work reported in this paper.

Data availability

Data will be made available on request.

Acknowledgment

We would like to thank J. Dorner and M. Fußeder from Max-Planck-Institut für Plasmaphysik for their technical support and especially to K. Hunger for diligent work on polishing the samples. We would like to thank Dr. M. Zibrov for providing on short notice tungsten (100) single crystals, that made this experiment possible.

This work has been carried out within the framework of the EUROfusion Consortium, funded by the European Union via the Euratom Research and Training Programme (Grant Agreement No 101052200 — EUROfusion). Views and opinions expressed are however those of the author(s) only and do not necessarily reflect those of the European Union or the European Commission. Neither the European Union nor the European Commission can be held responsible for them. The authors acknowledge the support from the Slovenian Research Agency (research core funding No. P2-0405 and research project No. J2-3038). The authors wish to acknowledge CSC – IT Center for Science, Finland, for computational resources. The authors acknowledge RADIATE project (Grant Agreement 824096 from the EU Research and Innovation programme HORIZON 2020) for TNA beam time approval and financing.

References

[1] L.C. Feldman, J.W. Mayer, S.T. Picraux, Materials Analysis by ion beam channeling, Academic Press, New York, 1982.
[2] W.-K. Chu, J.W. Mayer, M. Nicolet, Backscatering spectrometry, Academic press, San Diego, 1978.
[3] S.M. Myers, P.M. Richards, W.R. Wampler, F. Besenbacher, Ion-beam studies of hydrogen-metal interactions, J. Nucl. Mater. 165 (1989) 9–64.
[4] S.T. Picraux, F. Vook, Deuterium lattice location in Cr and W, Phys. Rev. Letters 33 (1974) 1216.
[5] S.T. Picraux, Defect trapping of gas atoms in metals, Nucl. Inst. Methods 182 (1981) 413–437.
[6] X. Jin, F. Djurabekova, E. A. Hodille, S. Markelj and K. Nordlund, "Analysis of lattice locations of deuterium in tungsten and its application for predicting deuterium trapping conditions," Phys. Rev. Mater. (under review), no. arXiv: 2312.09112 [cond-mat]., 2024.
[7] S. Zhang, et al., Simulation of Rutherford backscattering spectrometry from arbitrary atom structures, Phys. Rev. E 94 (2016) 043319.
[8] J. F. Ziegler, J. P. Ziegler and M. D. Biersack, SRIM - The Stopping and Range of Ions ion Matter, Chester, Maryland, USA: SRIM Co., 2008.
[9] ASTM Int'l E521-16, "Standard practice for neutron radiation damage simulation by charge-particle irradiation," in *Annual Book of ASTM Standards vol 12.02*, Philadelphia, PA, American Society for Testing and Materials, 2016, p. p 8.
[10] Z. Hu, et al., Effect of purity on the vacancy defects induced in self–irradiated tungsten: A combination of PAS and TEM, J. Nucl. Mater. 556 (2021) 153175.
[11] S. Wang, et al., Dynamic equilibrium of displacement damage defects in heavy-ion irradiated tungsten, Acta Mater. 244 (2023) 118578.
[12] B. Wielunska, et al., Dislocation structure of tungsten irradiated by medium to high-mass ions, Nucl. Fusion 62 (2022) 096003.
[13] S. Markelj, X. Jin, F. Djurabekova, J. Zavašnik, E. Punzón-Quijorna, T. Schwarz-Selinger, M. Crespillo, G. López, F. Granberg, E. Lu, K. Nordlund, A. Šestan, M. Kelemen, Unveiling the radiation-induced defect production and damage evolution in tungsten using multi-energy Rutherford backscattering spectroscopy in channeling configuration, Acta Mater. 263 (2024) 119499, https://doi.org/10.1016/j.actamat.2023.119499.
[14] T. Schwarz-Selinger, A critical review of experiments on deuterium retention in displacement-damaged tungsten as function of damaging dose, Mater. Res. Express 10 (2023) 102002.
[15] H.-D. Cabstanjen, Interstitial positions and vibrational amplitudes of hydrogen in metals investigated by fast ion channeling, Phys. Stat. Sol. (a) 59 (1980) 11–26.
[16] B. Wielunska, M. Mayer, T. Schwarz-Selinger, U. von Toussaint, J. Bauer, Cross Section Data for the D(^{3}He, p)^{4}He Nuclear Reaction from 0.25 to 6 MeV, Nucl. Instr. Meth. Phys. Res. B 371 (2016) 61.
[17] K. Nordlund, F. Djurabekova, G. Hobler, Large fraction of crystal directions leads to ion channeling, Phys. Rev. B 94 (2016) 214109.
[18] M. Meyer, "SIMNRA User's Guide, Report IPP 9/113," Max-Planck-Instutute für Plasmaphysik, Garching, Germany, 1997. [Online]. Available: http://www.rzg.mpg.de/~mam/.
[19] T. Schwarz-Selinger, A. Von Keudell, W. Jacob, Novel method for absolute quantification of the flux and angular distribution of a radical source for atomic hydrogen, J. Vac. Sci. Technol. A 18 (2000) 995–1001.
[20] M. Mayer, E. Gauthier, U.V. Toussaint, Quantitative depth profiling of deuterium up to very large depths, Nucl. Instr. Meth. Phys. Res. B 267 (2009) 506.
[21] X. Jin, et al., New developments in the simulation of Rutherford backscattering spectrometry in channeling mode using arbitrary atom structures, Modelling Simul. Mater. Sci. Eng. 28 (2020) 075005.
[22] S. Markelj, et al., Displacement damage stabilization by hydrogen presence under simultaneous W ion damage and D ion exposure, Nucl. Fus. 59 (2019) 086050.
[23] M. Pečovnik, S. Markelj, E. Hodille, T. Schwarz-Selinger, C. Grisolia, New rate equation model to describe displacement damage stabilization by hydrogen atoms in tungsten, Nuclear Fusion 60 (2020) 036024.
[24] J. Heikinheimo, et al., Direct observation of mono-vacancy and self-interstitial recovery in tungsten, APL Mater. 7 (2019) 021103.
[25] K. Heinola, T. Ahlgren, K. Nordlund, J. Keinonen, Hydrogen interaction with point defects in tungsten, Phys. Rev. B 82 (2010) 094102.
[26] N. Fernandez, Y. Ferro, D. Kato, Hydrogen diffusion and vacancies formation in tungsten: Density Functional Theory calculations and statistical models, Acta Mater. 94 (2015) 307–318.
[27] J. Hou, X.-S. Kong, X. Wu, J. Song, C.S. Liu, Predictive model of hydrogen trapping and bubbling in nanovoids in bcc metals, Nat. Mater. 18 (2019) 833–839.

[28] M. Pečovnik, T. Schwarz-Selinger, S. Markelj, Experiments and modelling of multiple sequential MeV ion irradiations and deuterium exposures in tungsten, J. Nucl. Mater. 550 (2021) 152947.
[29] Q. Yang, et al., A combined experimental and theoretical study of small and large vacancy clusters in tungsten, J. Nucl. Mater. 571 (2022) 154019.
[30] L.K. Walford, The X-ray Debye temperature of tungsten, Mat. Res. Bull. 4 (1969) 137–142.
[31] M.T. Weller, P.F. Henry, V.P. Ting, C.C. Wilson, Crystallography of hydrogen-containing compounds: realizing the potential of neutron powder diffraction, Chem. Commun. 21 (2009) 2973.